ALPHEUS

Results of experiments from model tests of initial PD design

D2.5.

Grant Agreement No.	883553
Start date of Project	01-04-2020
Duration of the Project	48 months
Deliverable Number	D2.5
Deliverable Leader	Chalmers
Dissemination Level	Public
Version	V1.0
Submission Date	24-03-2022
Authors	Håkan Nilsson, Chalmers Valery Chernoray, Chalmers

This project has received funding from the European Union's Horizon 2020 research and innovation programme under grant agreement No 883553.

Version #	Description	Author	Organisation	Date
0.1	First version based on material provided by: Petter Miltén, Valery Chernoray and Mikhail Tokarev	Håkan Nilsson	Chalmers	15-02-2022
0.2	2nd draft including CAD images, measurement details and operating conditions	Håkan Nilsson and Valery Chernoray	Chalmers	19-02-2022
1.0	Final version	Håkan Nilsson and Valery Chernoray	Chalmers	21-02-2022

Release Approval

Name	Role	Date
P-T. S., Storli	WP Leader	24-03-2022
J., Bricker	Technical Project Coordinator (TU Delft)	24-03-2022
D. Swierstra	Project Coordinator (TU Delft)	24-03-2022

Table of Contents

List of figures

List of tables

Executive Summary

This report presents the results of the PIV experiments of the positive displacement pump of the ALPHEUS project. An experimental test rig was set up at Chalmers, and measurements were performed using a PIV technique.

1. Introduction

ALPHEUS deliverable D2.5 should present the results of the experiments of the positive displacement (PD) pump of the ALPHEUS project. The deliverable is part of Task 2.3 “Multidisciplinary optimization of Positive Displacement RPT [M1-M24]”, where the descriptions related to the experiments are stated:
“An experimental test will be set up (2.3.2) and measurements will be performed at Chalmers using index matching PIV technique (2.3.3).”

The task has been completed, although not needing an index matching fluid. Regular tap water was found to be sufficient to give good experimental PIV data in combination with the used transparent materials.

Section 2 presents the experimental set-up. Section 3 presents the PIV results. Section 4 gives a short conclusion.

2. Experimental set-up

The design of the rig was developed in collaboration with the group at NTNU. The group at NTNU is responsible for the CFD simulations that should use the PIV results for validation. The collaboration ensured that the experiments were set up the best way.

Figure 1 shows the CAD geometry, supplied as a separate file that can be used to extract all the dimensions. The clearances between the rotor lobes and the top and bottom lids are approximately 0.5mm, given by a thin seal between those lids and the side walls (seen in red in the figure). The inlet and outlet diffusers were designed to get a more even velocity distribution for the PIV measurements.

The test rig is a closed-loop system, as shown in Figure 2, where the water goes from the bottom outlet of the test section, through a hose, through a flow meter, through a control valve, through an external pump, and back to the inlet of the test section. The external pump drives the flow through the test section when operating in turbine mode and is not used when operating in pump mode. The control valve is used to set the required head when operating in pump mode. The runner lobes are rotated by a motor and a gearbox that connects the rotation of the two rotors, making them rotate at exactly the same rotational speed but in opposite directions. An RPM sensor is used to monitor the rotational speed. Due to the small size of the test rig, the losses in the gear box and in the seals prevented the runner lobes from rotating in turbine mode, irrespectively of the head and flow rate. Thus, the motor had to be used also in turbine mode, to overcome those losses, and the rotational speed was varied over the region of interest. This has no effect on the PIV measurements, since the flow does not know if the runner lobes are rotating due to the forces from the flow or due to an external motor.

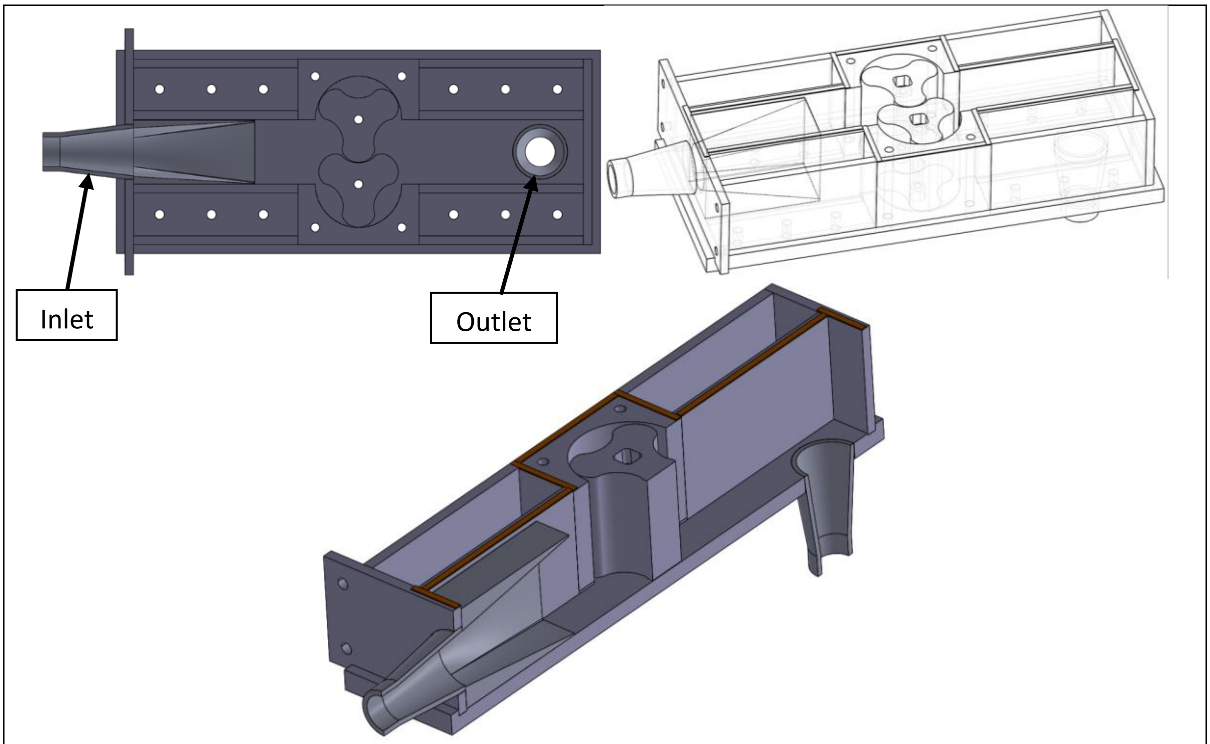

Figure 1 : CAD geometry.

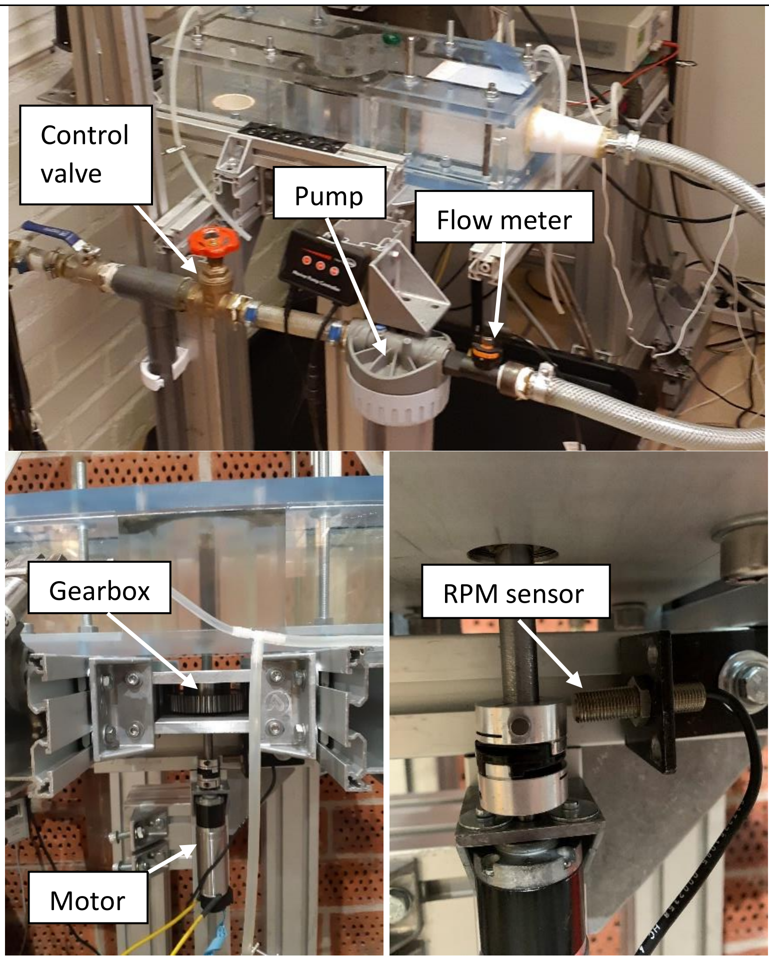

Figure 2 : Equipment for operating the rig.

Figure 3 shows the inlet and outlet diffusers that were designed to get a more even flow distribution, and the static pressure measurement hoses to get the static pressure difference over the test section.

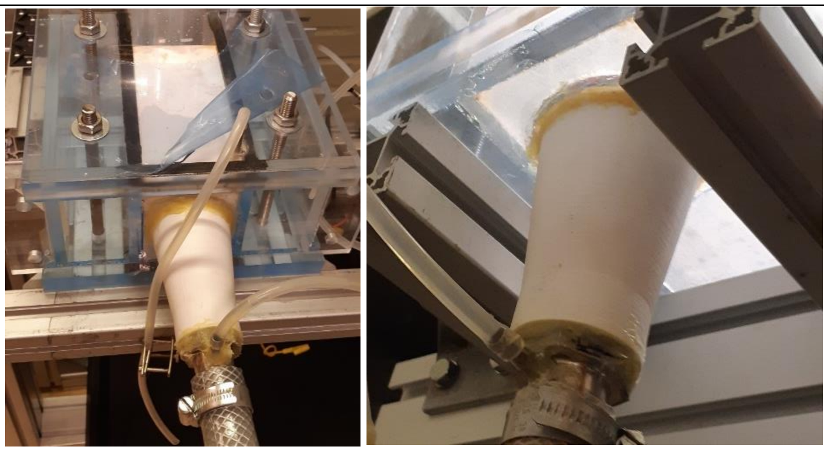

Figure 3 : Inlet and outlet diffusers, and static pressure measurement hoses.

Figure 4 shows the two-camera stereo PIV set-up, with a horizontal laser sheet entering at the left side of the pictures. One of the cameras is positioned perpendicular to the measurement plane and another camera is positioned at an angle of 30° with respect to the vertical axis. This way it was possible to use the first camera for additional 2D-2C (two-dimensional, two-component) measurements and the two cameras together were used for 2D-3C measurements. The cameras are 14-bit Imager Pro X 4 M with a 2048 × 2048 pixel sensor and 7.4 µm pixel dimension. The camera lenses (105-mm f/2.8 Sigma) were equipped with 570-nm low-pass filters to separate the fluorescent emission of the particles and the laser illumination. The planar illumination was performed by EverGreen 200 dual-cavity Nd-YAG laser with 532 nm wavelength. The laser was equipped with light-sheet forming optics, generating a horizontal light sheet with a thickness 2-3 mm. The fluid was regular tap water, which was found to have a sufficient index-matching with the transparent PMMA materials for the requested horizontal PIV plane through the test section. The laser sheet was able to penetrate the entire measurement section, including the runner lobes, without refractions out of the measurement plane. The water was seeded with 20-µm fluorescent Rhodamine B-based polystyrene particles. The fluorescent PIV was employed to avoid reflections from the metallic parts of the rig. The PIV calibration was carried out in situ, by placing a 2-plane calibration target inside the rig filled with water.

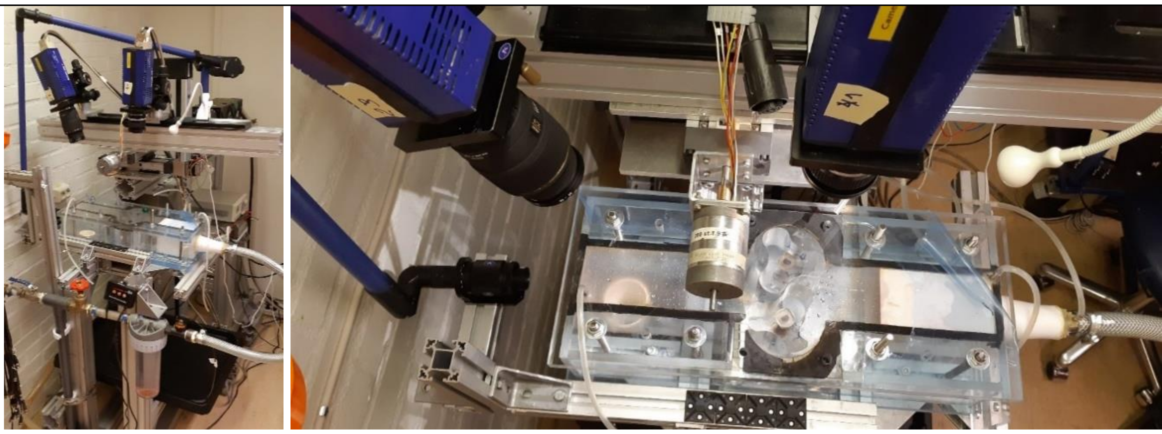

Figure 4 : Two-camera stereo PIV set-up.

The synchronization of the PIV system with the rotation of the rotor lobes was performed using a Hall effect sensor and a magnet mounted on the shaft of the motor, see Figure 2. An example of a particle image from one of the cameras is shown in Figure 5. The Davis 10 PIV software from LaVision was used for PIV processing. The processing steps included initial calibration with the calibration target, stereo self-calibration, stereoscopic reconstruction, cross-correlation and vector validation, vector statistics, and finally data masking. Vector statistics is obtained by phase-averaging of 100 images. The cross-correlation was performed in multipass procedure with decreasing window size in half. Initial interrogation window size was 64×64 pixels with 50 % overlap and final pass was performed with 32×32 pixels area size, 75 % overlap.

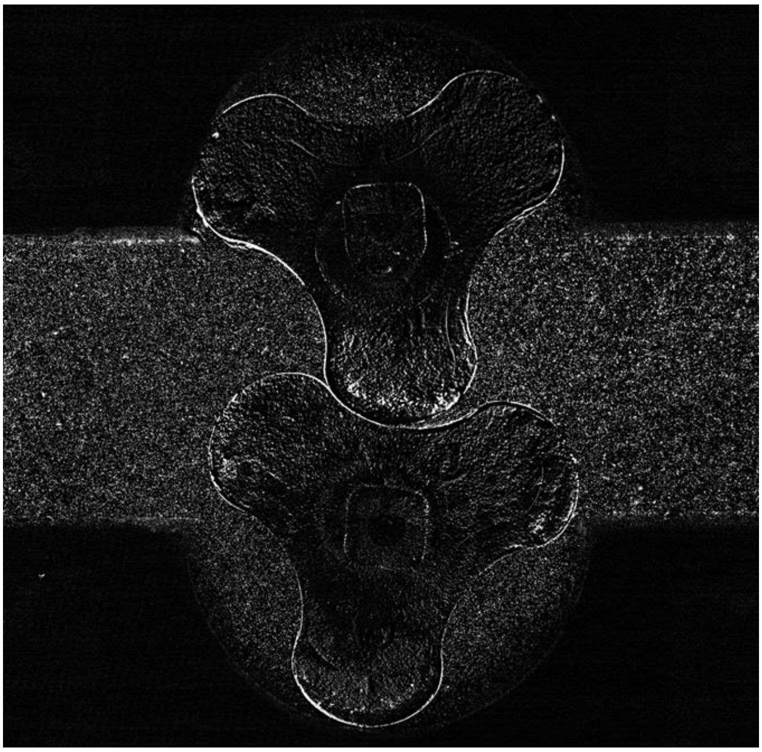

Figure 5 : Example of particle image

Table 1 shows details of the investigated cases, including RPM, flow rate (in LPM and m3/s) and pressure difference. The total and static pressure difference are the same since inlet and outlet pipes were of the same cross-section.

Mode	**RPM**	**Flow, LPM**	**Flow, m3/s**	**dP, Pa**	**dP tot, Pa**
Turbine 45 rpm	45	29.3	4.88E-04	-858	-858
Pump 45 rpm	45	11	1.83E-04	1058	1058
Pump 55 rpm	55	13	2.17E-04	1230	1230

Table 1 : Details of investigated cases

3. PIV results

The PIV results are here presented as images of the velocity magnitude distribution. In all the images the flow is from left to right, in both pump and turbine modes. The upper and lower runner lobes in the images are rotating in the clockwise and anti-clockwise, respectively, in both turbine and pump mode. The only difference is if the pressure difference between the inlet and outlet is supporting or counteracting the flow. The entire set of data is available in a separate file for further analysis during the validation of the numerical simulations.

3.1 Turbine mode

Figure 6 corresponds to a time-averaged field, given by an average of 100 samples obtained with 7.23Hz sampling frequency in turbine mode, running at 45 RPM. The total averaging time thus corresponds to about 10.4 runner lobe rotations. Due to the time averaging, the flow in the rotating lobe region is not relevant, and has been masked out of the figure. It can be noted that there is a non-uniform velocity distribution at the inlet, since the upper part to the left of (upstream) the runner lobes has higher velocities. The same is seen in the phased averaged data in the following figures in turbine mode, while it is much less pronounced in pump mode. There is no known reason for this behaviour.

Figures 7-9 show the phase-averaged velocity fields of the turbine mode, at 45 RPM runner lobe rotational speed. Each of those figures are phase-averaged at a particular rotational position of the runner lobes. The zero degree angle corresponds to when one of the lobes (the upper in the figures) is just “closing” the region that entraps the water between the lobe and the casing, at the upstream side. Further analysis of the results is left to when the results are further analysed during validation of CFD, and the results are simply shown here.

3.2 Pump mode

Figures 10-15 show the phase-averaged velocity fields of the pump mode. Figures 10-12 are results at 45 RPM runner lobe rotational speed and Figures 13-15 are results at 55 RPM runner lobe rotational speed. Each of those figures are phase-averaged at a particular rotational position of the runner lobes. The zero degree angle corresponds to when one of the lobes (the upper in the figures) is just “closing” the region that entraps the water between the lobe and the casing, at the upstream side. Further analysis of the results is left to when the results are further analysed during validation of CFD, and the results are simply shown here.

4. Conclusions

This report delivers the requested details on the experimental set-up and PIV results of the ALPHEUS positive displacement pump. Further analysis of the results is left to when the results are further analysed during validation of CFD, and the results are simply shown here. The complete CAD of the test section and the entire set of data are available in separate files.

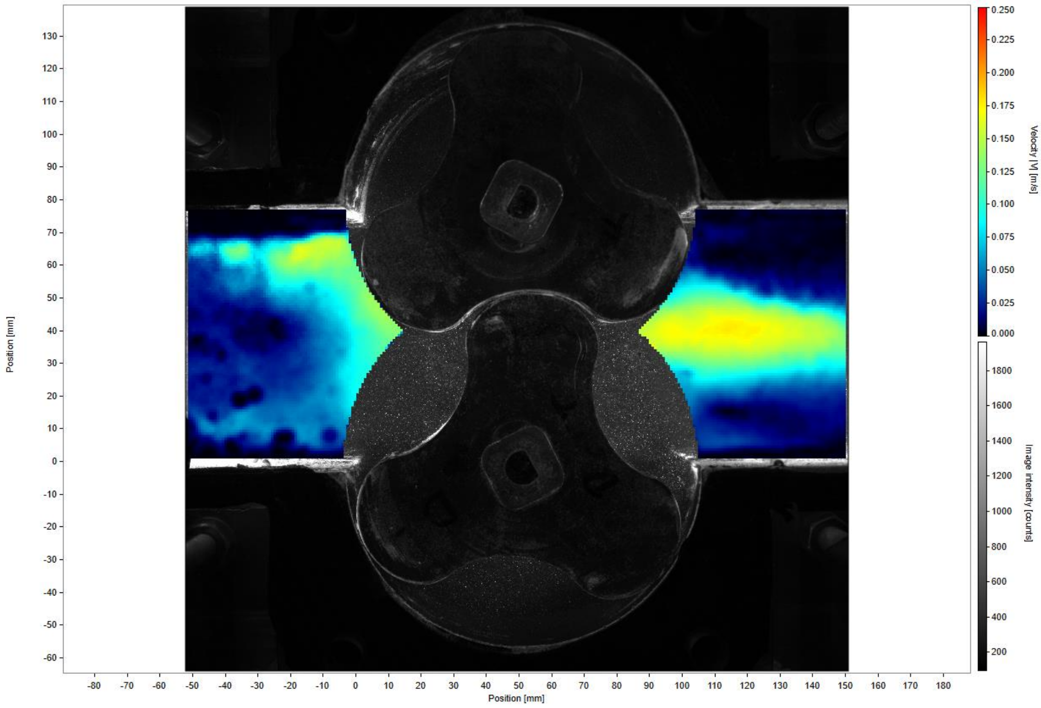

Figure 6 : Turbine mode, 45 RPM. Time-averaged velocity magnitudes.

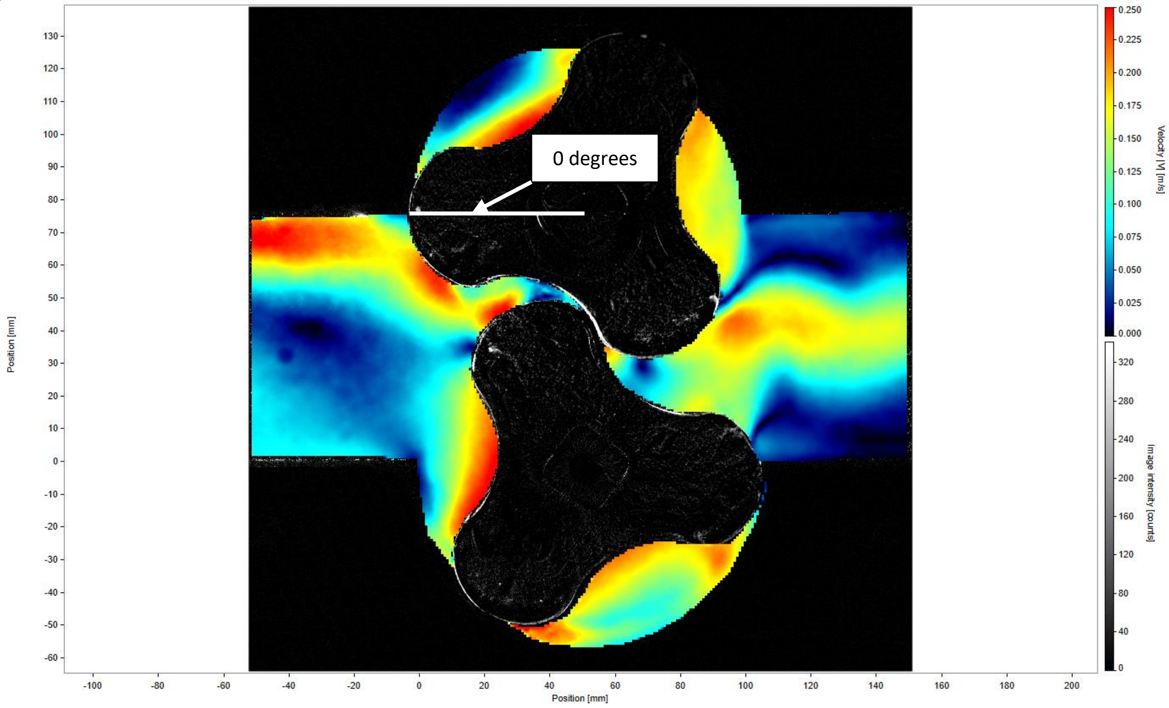

Figure 7 : Turbine mode, 45 RPM, Phase-averaged velocity magnitude at angle 0 degrees.

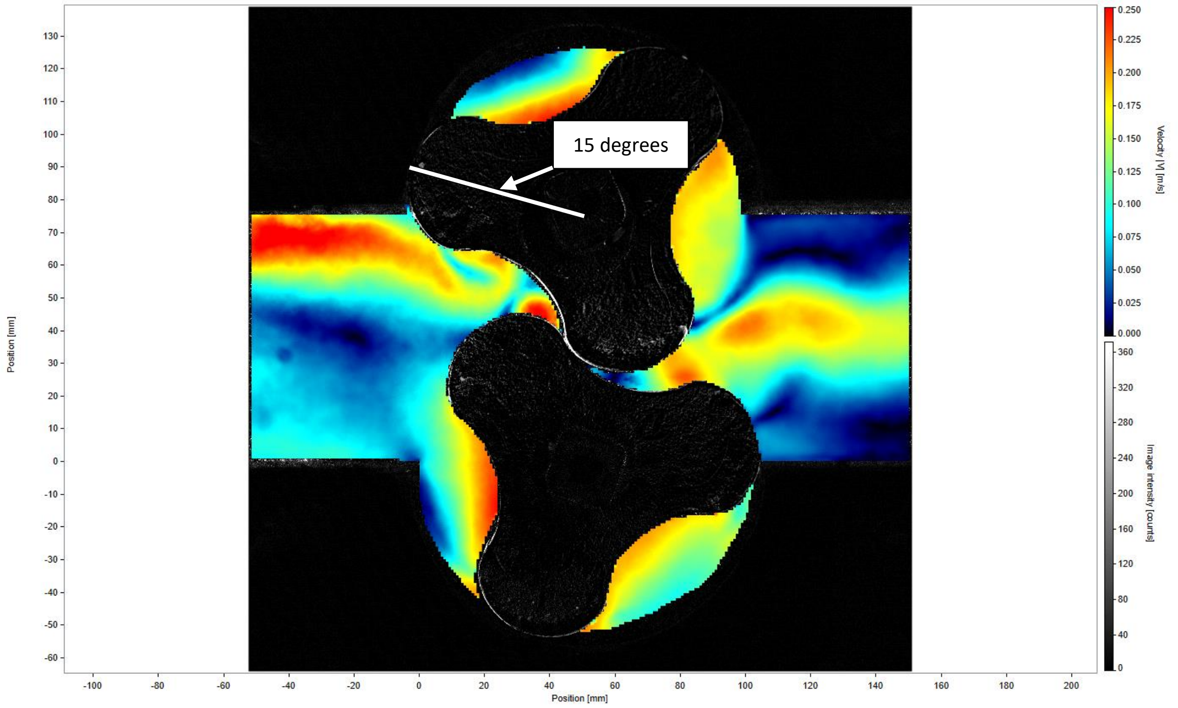

Figure 8 : Turbine mode, 45 RPM, Phase-averaged velocity magnitude at angle 15 degrees.

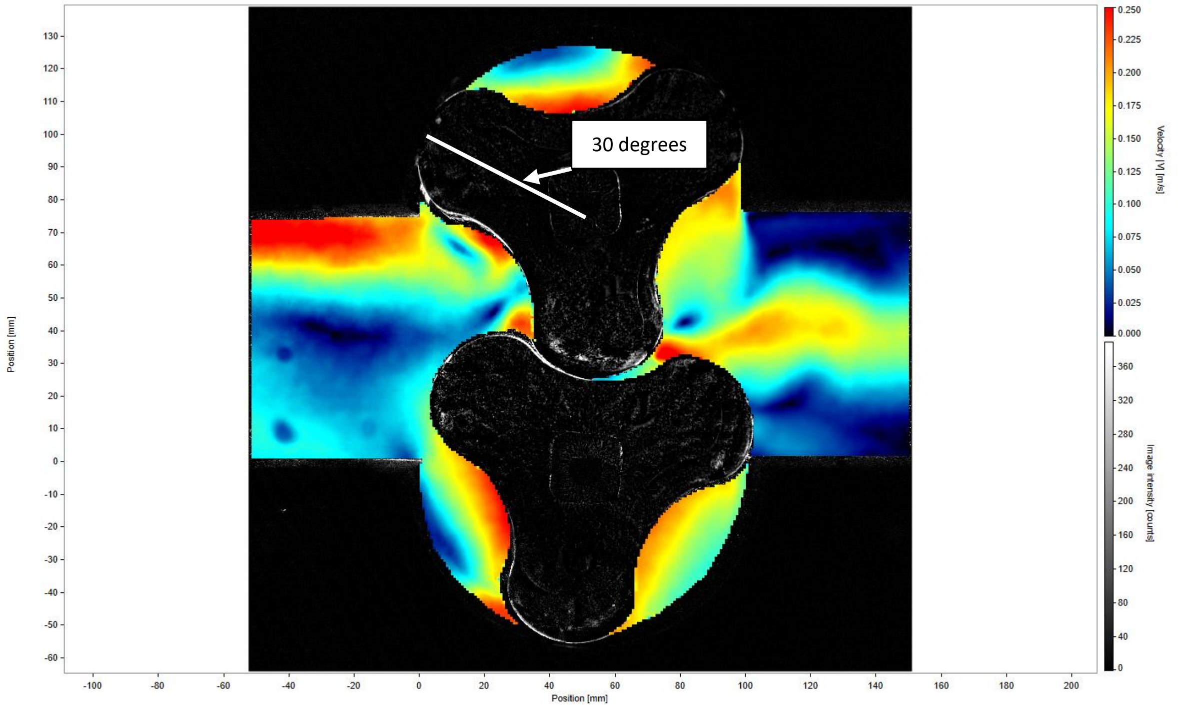

Figure 9 : Turbine mode, 45 RPM, Phase-averaged velocity magnitude at angle 30 degrees.

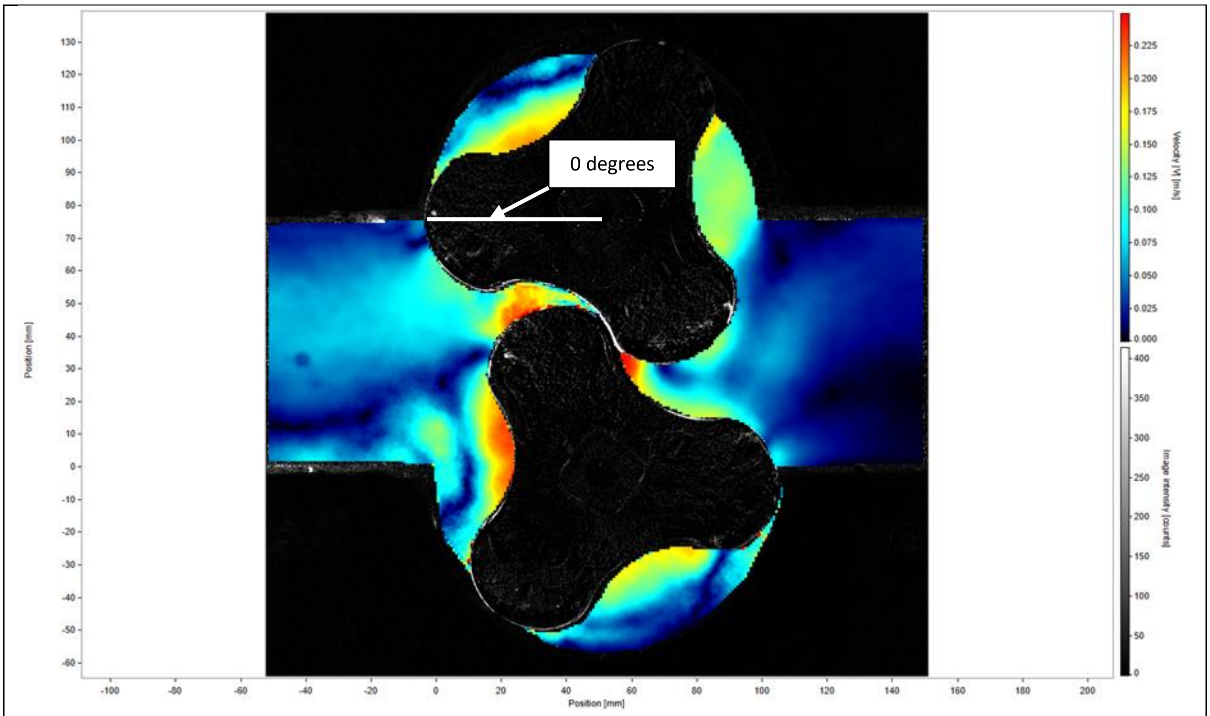

Figure 10 : Pump mode, 45 RPM, Phase-averaged velocity magnitude at angle 0 degrees.

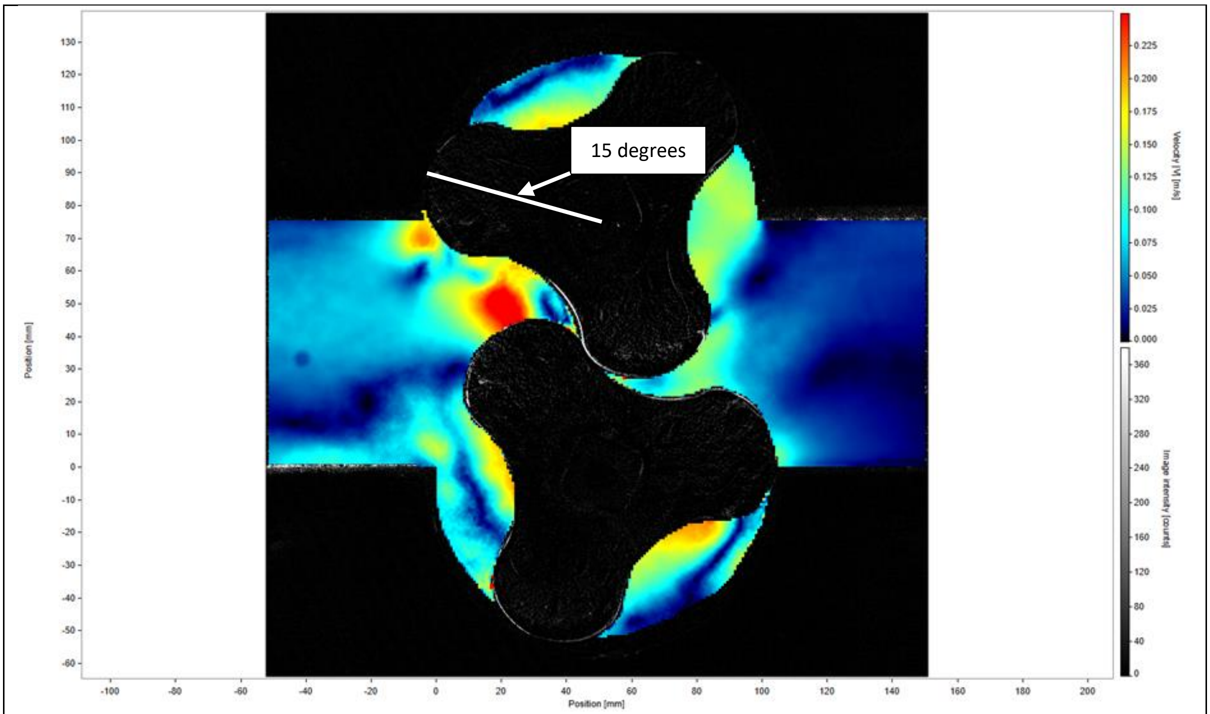

Figure 11 : Pump mode, 45 RPM, Phase-averaged velocity magnitude at angle 15 degrees.

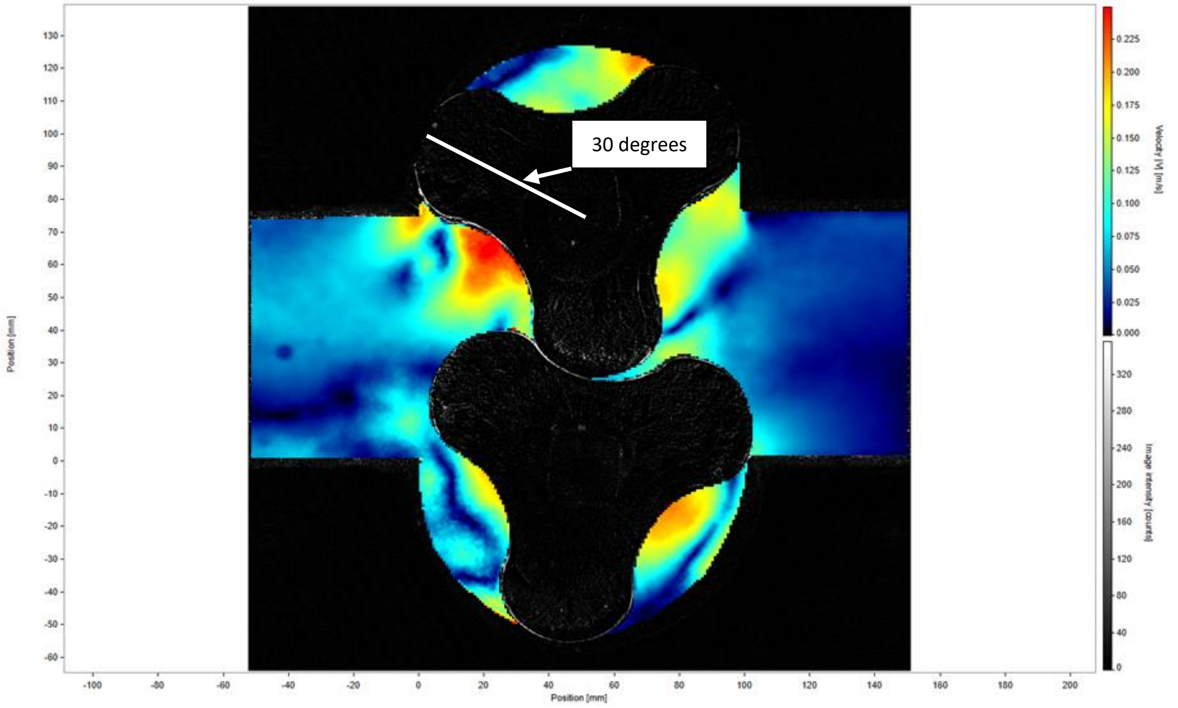

Figure 12 : Pump mode, 45 RPM, Phase-averaged velocity magnitude at angle 30 degrees.

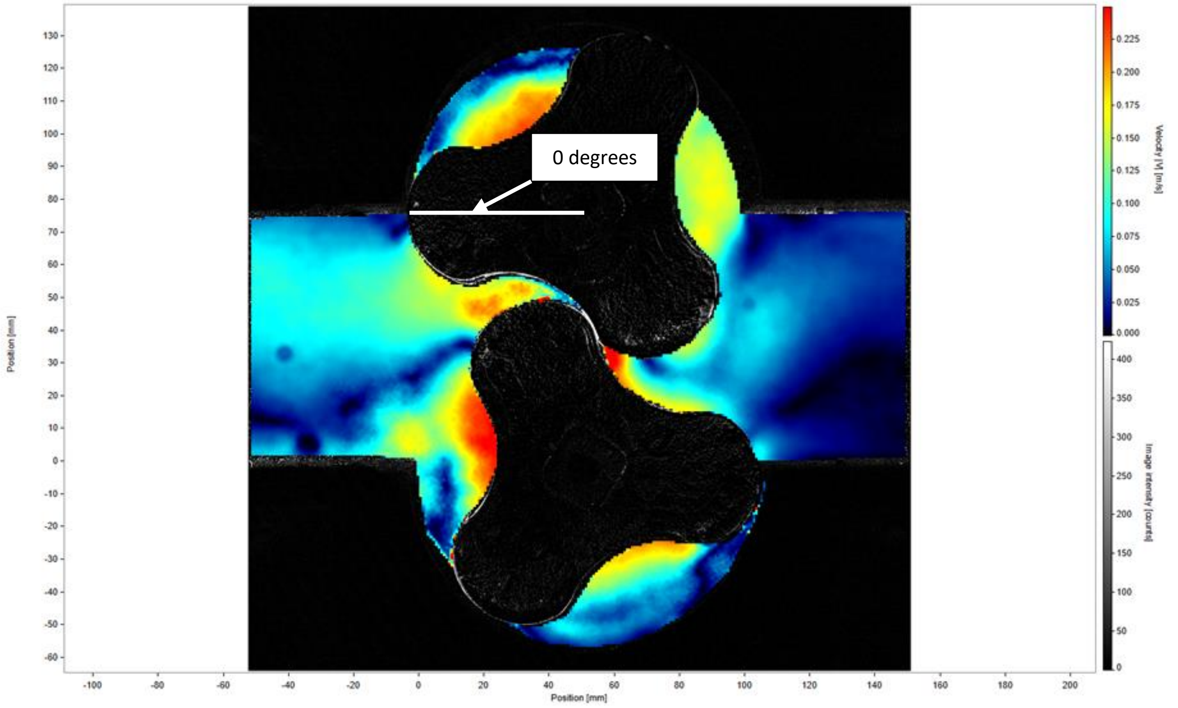

Figure 13 : Pump mode, 55 RPM, Phase-averaged velocity magnitude at angle 0 degrees.

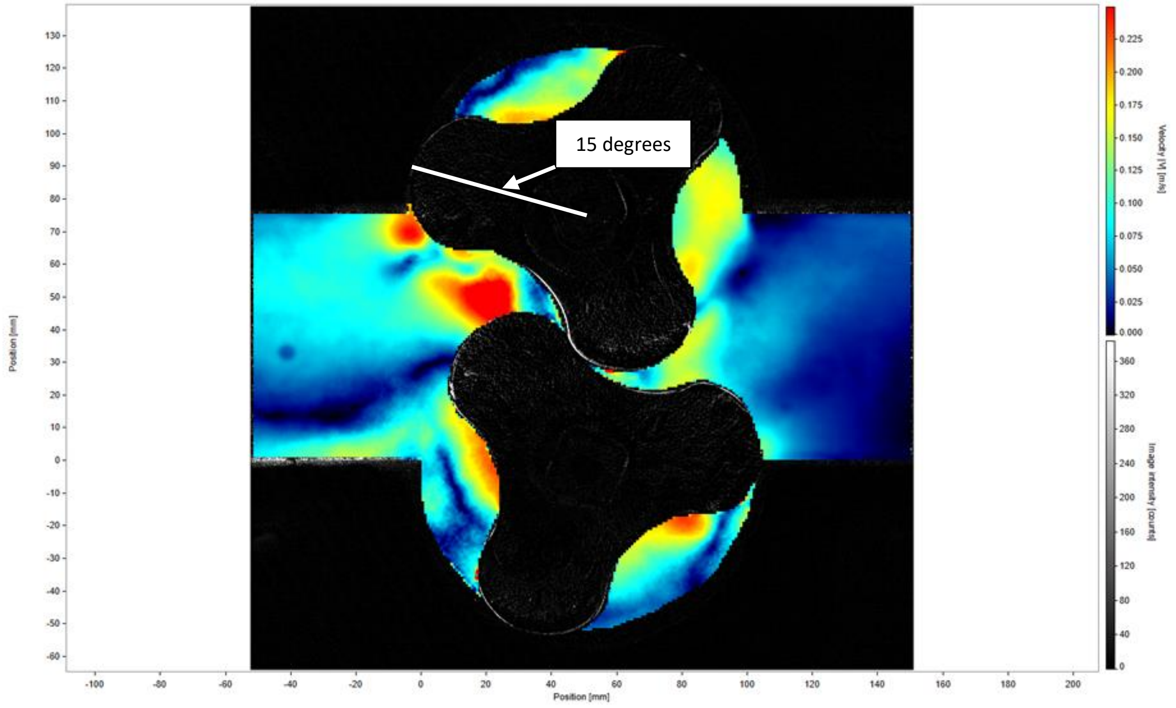

Figure 14 : Pump mode, 55 RPM, Phase-averaged velocity magnitude at angle 15 degrees.

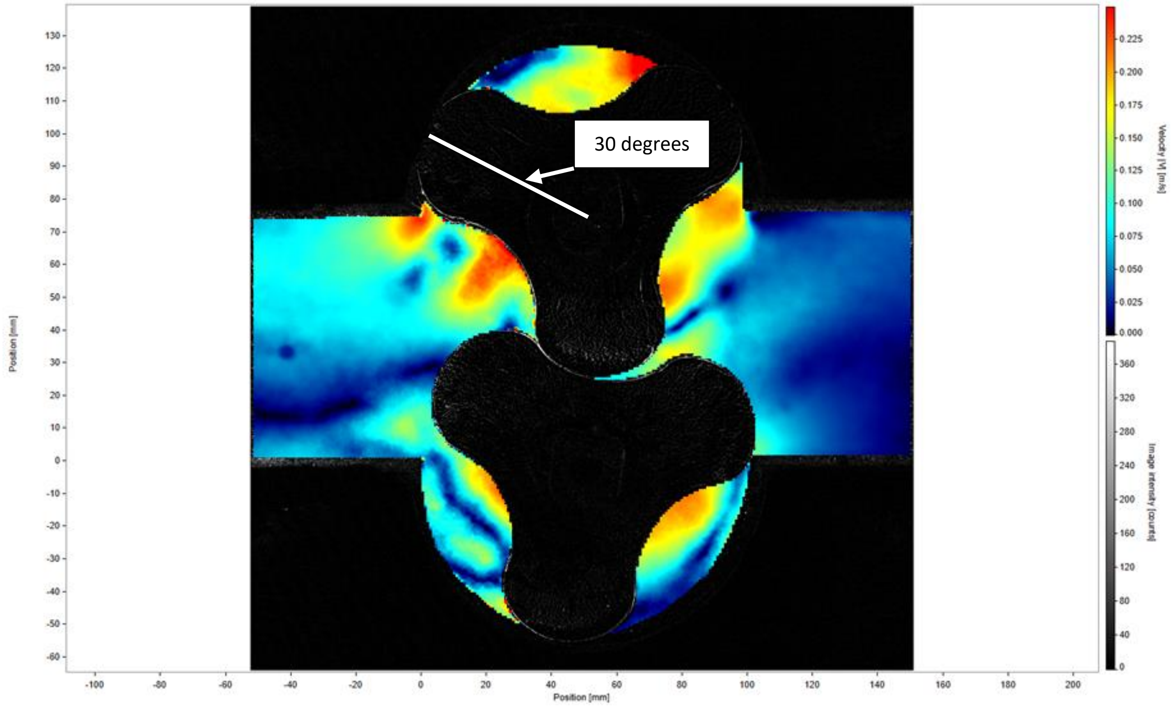

Figure 15 : Pump mode, 55 RPM, Phase-averaged velocity magnitude at angle 30 degrees.